KfK 2953
Mai 1980

A Model of Gas Cavity Breakup behind a Blockage in Fast Breeder Reactor Subassembly Geometry

Y. Fukuzawa
Institut für Reaktorentwicklung
Projekt Schneller Brüter

Kernforschungszentrum Karlsruhe

KERNFORSCHUNGSZENTRUM KARLSRUHE
Institut für Reaktorentwicklung
Projekt Schneller Brüter

KfK 2953

A Model of Gas Cavity Breakup behind a Blockage in Fast Breeder Reactor Subassembly Geometry

by

Y. Fukuzawa

Kernforschungszentrum Karlsruhe GmbH, Karlsruhe

Kernforschungszentrum Karlsruhe GmbH
ISSN 0303-4003

Abstract

A semi-empirical model has been developed to describe the transient behaviour of a gas cavity due to breakup behind a blockage in Liquid Metal Fast Breeder Reactor subassembly geometry. The main mechanisms assumed for gas cavity breakup in the present model are as follows:

- The gas cavity is broken up by the pressure fluctuation at the interface due to turbulence in the liquid.

- The centrifugal force on the liquid opposes breakup.

The model is able to describe experimental results on the transient behaviour of a gas cavity due to breakup after the termination of gas injection.

On the basis of the present model the residence time of a gas cavity behind a blockage in sodium is predicted and the dependence of the residence time on blockage size is discussed.

Zusammenfassung

Ein Modell zur Auflösung einer Gasansammlung hinter einer Blockade in einer Bündel-Geometrie ähnlich einem Schnell-Brüter-Brennelement

Um das transiente Verhalten einer Gasansammlung hinter einer Blockade in einer SNR 300 Bündelgeometrie während des Auflösungsvorgangs beschreiben zu können, wurde ein semi-empirisches Modell entwickelt. Die wichtigsten Mechanismen, die in dem vorgestellten Modell für die Gasauflösung vorausgesetzt wurden, sind folgende:

- Die Gasansammlung wird infolge Druckfluktuation an der Grenzschicht und durch Turbulenz in der Flüssigkeit aufgelöst.

- Die Zentrifugalkraft der Flüssigkeit wirkt der Auflösung entgegen.

Mit Hilfe des Modells ist es möglich, die experimentellen Ergebnisse bezüglich der Auflösung einer Gasansammlung nach Beendigung der Gaseinspeisung zu beschreiben. Auf der Basis des vorgestellten Modells wird die Verweilzeit einer Gasansammlung hinter einer Blockade in Natrium vorhergesagt und die Abhängigkeit der Verweilzeit von der Größe der Blockade diskutiert.

Contents

List of figures

1. Introduction

The phenomenon of gas bubble entrapment in the wake behind a blockage is considered to be one of the potential pin-to-pin failure propagation mechanisms due to fission gas release in the subassembly of a Liquid Metal Fast Breeder Reactor (LMFBR) [1].

Figure 1 shows the cross section of the subassembly with a corner blockage. A recirculating wake is formed behind the blockage and the temperatures in the wake are enhanced.

Hence, the possibility of fission gas release from fuel pins in the wake may be increased due to the high temperature. The released gas is accumulated in the wake, forming a gas cavity, and may cause a severe thermal effect on the fuel pins behind the blockage, i.e. dryout and melt.

The phenomenon of gas accumulation in the wake behind a blockage was inferred from gas injection experiments in full-scale 169-pin bundle with a 21 % planar corner blockage in sodium at Kernforschungszentrum Karlsruhe [2]. However, the information obtained from the experiments was not enough to fully describe the behaviour of gas in the wake, since the number and the position of bubble detectors, and hence data obtaind, were restricted. For this reason, gas injection experiments in water, of a half-bundle with the same pin arrangement and blockage size as in sodium, were performed to observe directly the behaviour of gas in the wake [3].

The experimental results in water showed that the gas was accumulated behind the blockage under some conditions of experiments, forming a gas cavity engulfing pins, and even after the termination of gas injection the cavity remained for a certain time. In order to predict the residence time of a gas cavity under various conditions of LMFBR an analytical approach is required.

The present report describes such a model which was developed semi-empirically. A comparison with experimental results is presented. The predicted residence time of a gas cavity in sodium and its dependence on blockage size, as a main parameter, are shown.

2. A Model

2.1 Background of the model

2.1.1 Recirculating wake

If a flow is partially blocked, a recirculating wake is formed behind the blockage. The main flow goes up from the separation point of the leading edge of the blockage to the stagnation point of the turning region of the flow. The recirculating wake is surrounded by the streamline from the separation to the stagnation points and blockage surface. The structure of the wake behind the blockage has been studied by various investigators, experimentally and theoretically.

Basmer et al. [4] showed visually a recirculating flow behind a blockage in water. The liquid in the wake circulates behind the blockage, representing an elliptical streamline.

Robinson [5] showed also visual wake behind a blockage in water. A transient eddy is observed at the boundary between main stream and recirculating wake.

The turbulence of the flow behind a blockage was measured by Judd [6] and calculated by Gregory and Lord [7]. In usual tube flow the intensity of turbulence (= I: Eq. (12)) has values in the neighbourhood of 0.01 ~ 0.1 [8]. However, Judd obtained a maximum turbulence of 0.3 (by his expression (= I^2)) behind a blockage in an air wind tunnel, which corresponded to the intensity of turbulence of 0.55. Also, Gregory and Lord obtained a maximum turbulence velocity of about 0.35 (by their expression (= $I/\sqrt{2}$)) behind a blockage, which corresponded to the intensity of turbulence of 0.5. The turbulence behind a blockage is much higher than that of usual tube flow. Their results showed that the maximum turbulence was at the boundary between main stream and recirculating wake.

These investigators also pointed out the influence of leakage flow through a blockage on the structure of the wake. The flow distribution and the turbulence in the wake are influenced by the magnitude and the type of leakage flows, i.e. homogeneous flow or discrete corner or central jets.

2.1.2 Gas cavity

The size of a gas cavity behind a planar corner blockage was measured in water under steady state conditions during gas injection and presented in [3]. In the lower velocity range of main flow the gas cavity extends over the whole wake region. With increasing velocity of the main flow the cavity size decreases. In the higher velocity range of the main flow the interface of gas cavity represents a circle. The gas cavity is broken up to small bubbles at the interface on the main stream side in the wake. By the breakup, the cavity decreases its size after the termination of gas injection.

2.2 Features of the model

On the basis of the experimental and theoretical results mentioned in section 2.1, a simple model is developed. A schematic diagram of the model is shown in Fig. 2, where the coolant flow is upwards. In the present model, the blockage type is limited to an impermeable blockage.

The main stream velocity increases in the axial direction of the subassembly due to the flow obstruction and reaches a maximum value at the leading edge of the blockage, then decreasing to the mean velocity in the subassembly. Corresponding to the change of the velocity, a static pressure decreases in the axial direction and has a minimum value at the blockage edge, then recovering.

The liquid in the wake goes down from the stagnation point of the top of the wake to the separation point of the blockage edge (i.e. reverse flow), then going into the main stream. Therefore, the liquid in a gap between the main stream and the reverse flow near the wall may rotate due to shear stress, forming a vortex. In the present report the existence of such a vortex is assumed and called a "central vortex". The central vortex is a limited region within the wake behind a blockage. In the case of a central blockage, the liquid goes down from the stagnation point to the edges of the blockage. Then the geometry of the central vortex behind the blockage may be a torus. In the case of corner blockage, the geometry of the vortex may be a 120° section of a torus (see Fig. 1). In the model, the blockage type is limited to a corner blockage. However, it may be easy to extend the model from the corner to the central blockage cases. The discussion on the central blockage case is made in Section 6.5.

The mass of liquid and momentum may be exchanged at the boundary between the main stream and the wake. The main stream velocity is much higher than the maximum reverse flow velocity near the wall. Also, the intensity of turbulence in the main stream is higher than that of the maximum reverse flow. Hence, the velocity and turbulence in the vortex on the main stream side may be different from those in the vortex on the subassembly wall side. In the present model, the central vortex is divided into two regions; Region 1 on the main stream side and Region 2 on the wall side. The velocity and turbulence of the flow in Region 1 of the vortex on the main stream side are higher than those in Region 2 on the wall side. The pressure and velocity of liquid in Region 1 of the vortex on the main stream side may fluctuate with time due to the high turbulence.

A gas cavity may be formed in the central vortex. The geometry of the cavity may be represented with the portion of the torus as the vortex geometry. The gas cavity is broken up to small bubbles in the vortex on the main stream side. Some of the produced bubbles go out and escape into the main stream. Others go with the liquid from Region 1 into Region 2 and may be absorbed into the cavity in Region 2 by the same mechanisms as the cavity is formed.

2.3 Assumptions of the model

The main mechanisms assumed for gas cavity breakup in the model are as follows:

Assumption 1: The gas cavity is broken up by the pressure fluctuations in the liquid due to the turbulence of the flow.

Assumption 2: The centrifugal force acting on the liquid opposes breakup of the cavity.

In addition to these assumptions the following assumption is made for the structure of the central vortex.

Assumption 3: The time-averaged angular velocity distribution of liquid is uniform, but the magnitude is different in each region of the vortex, on the main stream side and on the wall side.

2.4 Breakup mechanism in the model

On the basis of the assumptions, the mechanism of the cavity breakup is described. Figure 3 shows schematically the mechanism in the model.

The pressure fluctuation in the liquid due to the turbulence of the flow may disturb the interface of the cavity and cause ripples on the surface. The gas pressure in the cavity must be balanced by the time-averaged pressure of liquid at the interface.

Hence, if the pressure fluctuation of liquid is negative, the gas-liquid interface moves towards the liquid due to the pressure difference of gas and liquid in the radial direction, forming a ripple on the cavity surface. The ripple also moves in the tangential direction with the liquid flow. Then the ripple may be accelerated in the tangential direction due to the radial velocity gradient in the liquid and may be detached as a bubble by the inertia force of the liquid flow. Against these forces, surface tension opposes motion of the ripple radially outwards.

The liquid in the vortex is acted by the centrifugal force due to the curvature of the flow path, which may also oppose ripple growth and bubble detachment. The influence of the centrifugal force on ripple growth is schematically shown in Fig. 4. The liquid around a ripple moves locally outwards in the radial direction due to the centrifugal force, and then the gas-liquid interface of the ripple moves towards the gas cavity, resulting in opposition of ripple growth. In the present report, the force which opposes ripple growth, described above, is called a "centripetal force" acting on the ripple, which is caused by the centrifugal force acting on the liquid. Bubbles may be produced at the cavity surface on the main stream side, depending on the balance of these forces.

If the pressure fluctuation is positive, the interface moves towards the gas and may then produce a liquid-droplet by the momentum of the gas in the tangential direction or by the inertia of the liquid itself. However, the production rate of liquid-droplets may be much smaller than that of bubbles , because of the small inertia effect of gas on the liquid and also because of the low frequency of the relatively large fluctuations capable of causing the production of the droplet by the inertia of liquid itself. Hence, the cavity size is influenced markedly by the production of bubbles but not significantly by the production of liquid-droplets.

3. Central Vortex

3.1 Vortex radius

The radius of the central vortex depends on the size of the blockage. In this report, the vortex radius is assumed to satisfy the following relation.

$$\pi (2 r_w)^2 = \xi_w \cdot A_{Bf} \tag{1}$$

where r_w is the vortex radius, A_{Bf} is the blockage area (including the area of fuel pins) and ξ_w is a geometrical factor of the blockage which has the value 3 ($= \frac{360^o}{120^o}$) in the corner blockage case.

From Eq. (1), the vortex radius is expressed as follows:

$$r_w = \frac{1}{2}\sqrt{\frac{A_{Bf}\,\xi_w}{\pi}} \tag{2}$$

In the case of a 21 % corner blockage the vortex radius is 21 mm, obtained by Eq. (2).

3.2 Velocity distribution in the vortex

3.2.1 On the wall side

From the assumption of uniform angular velocity distribution, the tangential velocity of liquid in Region 2 of the vortex on the wall side is expressed as a function of the radial position as follows:

$$v = r \cdot \frac{v_u}{r_w} \tag{3}$$

where v_u is the reverse flow velocity near the subassembly wall.
The reverse flow velocity may be related to the main flow velocity as follows:

$$v_u = \varepsilon \cdot v_0 \tag{4}$$

where v_0 is the main flow velocity and ε is the ratio of the reverse flow velocity to the main flow velocity, which is about 0.3 in the case of a 21 % planar corner blockage in water [3] (see Section 6.3).

From Eqs. (2), (3) and (4), the velocity distribution in Region 2 of the vortex on the wall side is expressed as follows:

$$v = \left(2\varepsilon \cdot \sqrt{\frac{\pi}{A_{Bf}\, \xi_w}}\right) \cdot v_0\, r \tag{5}$$

3.2.2 On the main stream side

From the assumption of uniform angular velocity distribution, the time-averaged tangential velocity of liquid in Region 1 of the vortex on the main stream side is expressed as follows:

$$\bar{v} = r \cdot \frac{v_d}{r_w} \tag{6}$$

where v_d is the velocity at the boundary between main stream and wake. The velocity of the main stream increases along the axial position of the subassembly due to the flow obstruction, reaching a maximum value at the blockage position, then decreasing in the downstream direction to the mean flow velocity. The velocity at the boundary between the main stream and the wake increases with increasing velocity at the throat outside of the blockage. Thus, the velocity at the boundary may be approximately expressed as follows:

$$v_d = \frac{1}{2}\left(v_0 + v_t\right) \tag{7}$$

where v_t is the velocity at the throat outside of the blockage, which is expressed as follows:

$$v_t = \frac{v_0}{1 - \frac{A_{Bf}}{A_{of}}} \tag{8}$$

where A_{of} is the total area of the cross section of the subassembly (including the area of fuel pins). The velocity at the boundary is then

$$v_d = v_0 \cdot \frac{1 - \frac{A_{Bf}}{2\,A_{of}}}{1 - \frac{A_{Bf}}{A_{of}}} \tag{9}$$

From Eqs. (2), (6) and (9), the time-averaged tangential velocity distribution of liquid in Region 1 of the vortex on the main stream side is expressed as follows:

$$\bar{v} = \left(\frac{2 - \frac{A_{Bf}}{A_{of}}}{1 - \frac{A_{Bf}}{A_{oP}}} \cdot \sqrt{\frac{\pi}{A_{Bf}\, \varepsilon_w}} \right) \cdot v_0 r \tag{10}$$

3.3 Pressure fluctuation

The velocity of liquid in Region 1 of the vortex on the main stream side fluctuates with time due to the turbulence of the flow. Then the velocity is expressed as follows:

$$v = \bar{v} + \delta v \tag{11}$$

where δv is the velocity fluctuation and then

$$\delta v \gtrless 0$$

The intensity of turbulence is generally expressed as follows:

$$I = \frac{\sqrt{\overline{\delta v^2}}}{\bar{v}} \tag{12}$$

where $\sqrt{\overline{v^2}}$ is the root-mean-square value of the velocity fluctuation.

The pressure of liquid in Region 1 also fluctuates with time and is expressed as follows:

$$P_l = \bar{P}_l + \delta P \tag{13}$$

where $\bar{P}_l$ is the time-averaged pressure and δP is the pressure fluctuation, then

$$\delta P \gtrless 0$$

A relation between pressure and velocity fluctuations is expressed as follows:

$$\sqrt{\overline{\delta P^2}} = k_M \rho_l \left(\sqrt{\overline{\delta v^2}} \right)^2 \tag{14}$$

where $\sqrt{\overline{\delta p^2}}$ is the root-mean-square value of the pressure fluctuation and k_{p1} is constant which is about 0.7 in the higher range of Reynolds number [9]. From Eqs. (12) and (14) the following equation is obtained.

$$\sqrt{\overline{\delta p^2}} = k_{p1} \cdot I^2 \cdot \rho \, \bar{v}^2 \tag{15}$$

If the intensity of turbulence I is constant, equation (15) is rewritten as follows:

$$\sqrt{\overline{\delta p^2}} = k_p \cdot \rho \, \bar{v}^2 \tag{16}$$

where k_p is constant and

$$k_p \equiv k_{p1} \cdot I^2 \tag{17}$$

From Eq. (16) the magnitude of the root-mean-square value of the pressure fluctuation can be estimated. For a main flow velocity of 4 m/s in water, the maximum magnitude is about 3×10^3 N/m^2, which is obtained from Eq. (16) using Eq. (10) for $r = r_w$ and using $I = 0.5$ and $k_{p1} = 0.7$.

4. Breakup of Gas Cavity

4.1 Related forces

The pressure fluctuation in the liquid due to the turbulence of the flow may disturb the interface of the cavity and cause ripples on the surface (see Fig. 3). By using the root-mean-square value of the fluctuation the mean magnitude of the force acting on the ripple due to the fluctuation may be expressed as follows:

$$F_p = \sqrt{\overline{\delta P^2}} \cdot \left\{ \pi \left(\frac{d_b}{2} \right)^2 \right\} \tag{18}$$

where d_b is the diameter of the bubble which is produced by the ripple. The ripple moves in the radial direction and also moves in the tangential direction with the liquid flow. Then the ripple is accelerated in the tangential direction due to the radial velocity gradient in the liquid and detached as a bubble by the inertia force of the liquid flow. The velocity difference of the liquid in the radial distance of d_b is

$$\Delta \bar{v} = d_b \cdot \frac{\bar{v}_d}{r_w} \tag{19}$$

Then the inertia force which accelerates the ripple in the tangential direction is expressed as follows:

$$F_i = \rho_\ell \left(d_b \frac{\bar{v}_d}{r_w} \right)^2 \cdot \left\{ \pi \left(\frac{d_b}{2} \right)^2 \right\} \tag{20}$$

Against these forces, surface tension and the centripetal force oppose motion of the ripple radially outwards. The force due to the surface tension is expressed as follows:

$$F_s = \frac{4\sigma}{d_b} \cdot \left[\pi \left(\frac{d_b}{2} \right)^2 \right] \tag{21}$$

where σ is the surface tension. The centripetal force acting on the ripple, caused by the centrifugal force on the liquid, is expressed as follows:

$$F_c = \rho_\ell \frac{\bar{v}^2}{r_c} \cdot \left[\frac{4}{3} \pi \left(\frac{d_b}{2} \right)^3 \right] \tag{22}$$

where r_c is the cavity radius.

4.2 Breakup rate

From the description of breakup mechanism in Section 2.4 the volumetric breakup rate per unit area of the cavity surface may be expressed as follows:

$$(\nabla_b)_0 = f_1\left(\sqrt{\overline{\delta P^2}}\ ,\ \bar{v}\ ,\ \sigma\ ,\ r_c\ ,\ d_b\right) \tag{23}$$

where f is an arbitrary function. A dimensional analysis of these variables gives the following relationship of dimensionless groups (see Section 6.1):

$$\frac{(\nabla_b)_0}{\bar{v}} = f_2\left(\frac{d_b\sqrt{\overline{\delta P^2}}}{\sigma}\ ,\ \frac{d_b}{r_c}\right) \tag{24}$$

By using an index, the arbitrary function is expressed as follows:

$$\frac{(\nabla_b)_0}{\bar{v}} \equiv k\left(\frac{d_b\sqrt{\overline{\delta P^2}}}{\sigma}\right)^{m_b}\left(\frac{d_b}{r_c}\right)^{n_b} \tag{25}$$

where k, m_b and n_b are constants. From Eq. (16) equation (25) is rewritten as follows:

$$(\nabla_b)_0 = k_b\,\bar{v}\left(\frac{\rho_l\,\bar{v}^2 d_b}{\sigma}\right)^{m_b}\left(\frac{d_b}{r_c}\right)^{n_b} \tag{26}$$

where $$k_b \equiv k\,(k_p)^{m_b}$$

The total breakup rate is expressed as follows:

$$\nabla_b = \frac{A_t\,\xi_f}{\xi_w\,\xi_b}\,(\nabla_b)_0 \tag{27}$$

where ξ_f is the ratio of gas-liquid interface area to the total surface area of the cavity which includes the fuel pins, A_t is the surface area of the torus and ξ_b is the geometrical factor of the cavity surface for the breakup for which a value of 3 is adopted in the present model (see Section 6.3). The surface area of the torus is expressed as follows:

$$A_t = 4\pi^2 r_w r_c \tag{28}$$

From Eqs. (26) to (28), the following equation is obtained.

$$V_b = \xi_f \left(\frac{4\pi^2 r_w r_c}{\xi_w \xi_b}\right) k_b \cdot \bar{v} \left(\frac{\rho_\ell \bar{v}^2 d_b}{\sigma}\right)^{m_b} \left(\frac{d_b}{r_c}\right)^{n_b} \tag{29}$$

By using Eqs. (2) and (10) for $r = r_c$, equation (29) is transformed as follows:

$$V_b = \xi_f k_b \psi_{b1} \psi_{b2} \psi_{b3} (v_0)^{1+2m_b} (r_c)^{2+2m_b-n_b} \tag{30}$$

where $$\psi_{b1} \equiv \left(\frac{\rho_\ell}{\sigma}\right)^{m_b}$$

$$\psi_{b2} \equiv (d_b)^{m_b+n_b}$$

$$\psi_{b3} \equiv \left(\frac{4\pi^2}{\xi_w \xi_b}\right)\left(\frac{4\pi}{A_{Bf}\xi_w}\right)^{m_b}\left(\frac{1-\frac{A_{Bf}}{2A_{of}}}{1-\frac{A_{Bf}}{A_{of}}}\right)^{1+2m_b}$$

and where ψ_{b1} is a function of the physical properties, ψ_{b2} a function of the diameter of produced bubbles and ψ_{b3} a function of the blockage geometry. As shown in Eq. (30) the breakup rate was expressed as a function of physical properties, bubble diameter, blockage size, main flow velocity and cavity radius.

The values of k_b, m_b and n_b must be determined on the basis of experiments. A comparison with experimental results is made for the determination of these constants in Section 5.

4.3 Transient behaviour

From the mass continuity of gas the transient behaviour of a cavity after the termination of gas injection is described by the following equation.

$$(\rho_g)_c \frac{A_t \xi_f}{\xi_w}\left(-\frac{dr_c}{dt}\right) = (\rho_g)_d \cdot V_b - (\rho_g)_u V_{ab} \tag{31}$$

where $\frac{dr_c}{dt}$ is the rate of change of the cavity radius with time, $(\rho_g)_c$ is the gas density in the cavity, $(\rho_g)_d$ and $(\rho_g)_u$ are the gas densities of the bubbles in Regions 1 and 2 of the vortex on the main stream side and on the wall side, respectively, and V_{ab} is the re-absorption rate of bubbles into the cavity. Assuming that $(\rho_g)_c = (\rho_g)_d = (\rho_g)_u$, the following equation is obtained from Eq. (31).

$$\frac{A_t \varepsilon_f}{\varepsilon_w}\left(-\frac{dr_c}{dt}\right) = V_b - V_{ab} \tag{32}$$

Some of the bubbles produced by the breakup in Region 1 of the vortex on the main stream side go into Region 2 on the wall side, being re-absorbed into the cavity, and others escape from the wake into the main stream, as mentioned in Section 2. The re-absorption rate depends on the breakup rate and on the velocity distribution in the wake, especially on the reverse flow velocity on the wall side. In the model the re-absorption rate is assumed to depend on the ratio of the tangential flow rate of the liquid in Regions 1 and 2, being expressed as follows:

$$V_{ab} = V_b \cdot \frac{\int_r^{r_w} (v)_u \, dr}{\int_r^{r_w} (\bar{v})_d \, dr}$$

$$= V_b \cdot \frac{\bar{v}_u}{\bar{v}_d} \tag{33}$$

By using Eqs. (4) and (9), the re-absorption rate is rewritten as follows:

$$V_{ab} = \zeta V_b$$

where

$$\zeta = \varepsilon \cdot \frac{1 - \frac{A_{Bf}}{A_{of}}}{1 - \frac{A_{Bf}}{2A_{of}}} \tag{34}$$

For a 21 % corner blockage, ζ is about 0.27. From Eqs. (32) and (33) the following equation is obtained.

$$\frac{A_t \xi_f}{\xi_w}\left(-\frac{dr_c}{dt}\right) = (1-\zeta)\cdot V_b \tag{35}$$

From Eqs. (28), (30) and (35), the rate of change of the cavity radius is expressed as follows:

$$-\frac{dr_c}{dt} = \frac{\xi_w(1-\zeta)k_b\psi_b}{4\pi^2 r_w}(v_0)^{1+2m_b}(r_c)^{1+2m_b-n_b} \tag{36}$$

where $\psi_b \equiv \psi_{b1}\psi_{b2}\psi_{b3}$

Assuming that $2m_b - n_b \neq 0$ and integrating Eq. (36), the following equation is obtained for the cavity radius.

$$r_c = \left[r_i^{n_b-2m_b} + \frac{(2m_b-n_b)\xi_w(1-\zeta)k_b\psi_b}{4\pi^2 r_w}(v_0)^{1+2m_b}\cdot t\right]^{\frac{1}{n_b-2m_b}} \tag{37}$$

where t is the time and r_i is the initial radius of the cavity at t=0. Equation (37) represents the cavity radius as a function of time after the termination of gas injection.

5. Comparison with Experimental Results

5.1 Change of cavity radius with time

For constant v_0 the following relation is obtained from Eq. (36).

$$y = \alpha_b \cdot x \tag{38}$$

where

$$y \equiv \ln \left[\frac{\left(-\frac{dr_c}{dt}\right)_2}{\left(-\frac{dr_c}{dt}\right)_1} \right]$$

$$x \equiv \ln \left[\frac{(r_c)_2}{(r_c)_1} \right]$$

where the suffixes 1, 2 represent values at times t_1 and t_2 and where

$$\alpha_b \equiv 1 + 2m_b - n_b \tag{39}$$

A value of α_b is obtained by a comparison of the calculation by Eq. (38) with experimental results using data presented in [3]. The data are plotted in Fig. 5, and give some support to the linear relationship predicted by Eq. (38), suggesting that the model takes account of the important mechanisms. From the figure a value of about 2 is obtained for α_b. Then the following relation is obtained from Eq. (39).

$$2m_b - n_b \simeq 1 \tag{40}$$

By using Eq. (40), equation (37) is rewritten as follows:

$$\Sigma = \beta_b t \tag{41}$$

where

$$\Sigma = \frac{1}{r_c} - \frac{1}{r_i}$$

$$\beta_b \equiv \frac{\xi_w (1-S) k_b \psi_b}{4\pi^2 r_w} (v_0)^{1+2m_b} \tag{42}$$

From Eq. (42) the following relation is obtained

$$\ln\left[\frac{(\beta_b)_2}{(\beta_b)_1}\right] = (1+2m_b)\,\ln\left[\frac{(v_0)_2}{(v_0)_1}\right] \tag{43}$$

for the coefficient $(\beta_b)_1$ and $(\beta_b)_2$ at main flow velocities $(v_0)_1$ and $(v_0)_2$ respectively. In order to obtain values of β_b a comparison is made of the calculation by Eq. (41) with experimental results using data which were presented in [3]. Data obtained in experiments at flow velocities of 2 m/s and 3 m/s are plotted in Fig. 6. The data at 2 m/s is consistent with the linear relationship predicted by Eq. (41), within the limits of experimental uncertainty, and suggest a value for β_b of ~ 6×10^{-3} (1/s·mm). The data for 3 m/s is very limited. If a linear relationship is assumed a rough value of β_b of about 3×10^{-2} is indicated. By using these values the following relation is obtained from Eq. (43).

$$\begin{aligned} 1 + 2m_b &= \frac{\ln\left(\frac{3\times10^{-2}}{6\times10^{-3}}\right)}{\ln\left(\frac{3}{2}\right)} \\ &= 3.969\cdots \\ &\simeq 4. \end{aligned} \tag{44}$$

Then the following values are obtained from Eqs. (40) and (44).

$$m_b \simeq \frac{3}{2} \quad , \qquad n_b \simeq 2 \tag{45}$$

Therefore, the breakup rate is expressed as follows:

$$\nabla_b = \left(\frac{A_t \xi_f}{\xi_w \xi_b}\right) k_b \bar{v} \left(\frac{\rho_e \bar{v}^2 d_b}{\sigma}\right)^{\frac{3}{2}} \left(\frac{d_b}{r_c}\right)^2 \tag{46}$$

or

$$\nabla_b = \xi_f k_b \psi_{b1} \psi_{b2} \psi_{b3} (v_0)^4 (r_c)^3 \tag{47}$$

where $$\psi_{b1} = \left(\frac{\rho_\ell}{\sigma}\right)^{\frac{3}{2}} \tag{48}$$

$$\psi_{b2} = \left(d_b\right)^{\frac{7}{2}} \tag{49}$$

$$\psi_{b3} = \left(\frac{4\pi^2}{\xi_w \xi_b}\right)\left(\frac{4\pi}{A_{Bf}\,\xi_w}\right)^{\frac{3}{2}}\left(\frac{1 - \frac{A_{Bf}}{2A_{of}}}{1 - \frac{A_{Bf}}{A_{of}}}\right)^4 \tag{50}$$

Also, the change of cavity radius with time is expressed as follows:

$$\frac{1}{r_c} = \frac{1}{r_i} + \frac{\xi_w (1-\varepsilon) k_b \psi_b}{4\pi^2 r_w} (v_0)^4 t \tag{51}$$

To obtain experimentally a value of k_b as well as m_b and n_b, a comparison is made of the calculation by Eq. (51), using various values of k_b, with experimental results of the change of cavity radius, using data from [3]. Figure 7 shows the comparison for the determination of k_b where the calculation used $\xi_w = 6$ $(= \frac{360^\circ}{60^\circ})$ because of the half-bundle of the test section. It is assumed that the diameter of bubbles produced by the breakup process is equal to the gap distance between fuel pins (1.9 mm). In this case the figure suggests a value of $\sim 4 \times 10^{-4}$ for k_b.
By using these values of k_b, m_b and n_b obtained in the previous figures, the transient behaviour of a gas cavity may be predicted by the present model. The comparison of the change of cavity radius between calculational and experimental results is shown in Fig. 8. It may be seen that the calculation is consistent with the few experimental results available.

5.2 Residence time

The residence time of gas cavity is defined as the life time of the cavity from the termination of gas injection to its disappearance [3]. The gas cavity is defined as a stationary bubble with a radius larger than two times the hydraulic radius of the subchannel (2.7 mm) [3]. Then the residence time is expressed from Eq. (51) as follows:

$$\tau = \frac{1}{\beta_b}\left(\frac{1}{2r_k} - \frac{1}{r_i}\right) \tag{52}$$

where r_ℓ is the hydraulic radius of the sub-channel and

$$\beta_b = \frac{\xi_w (1-\varepsilon) k_b \psi_b}{4\pi^2 r_w} (v_0)^4$$

A comparison between calculated and measured residence times is shown in Figs. 9 and 10 for different gas injection rates before the termination, where data were also obtained from [3]. Experimental values of the initial radius of the cavity were used for the calculation since the size depended on the main flow velocity and on the gas injection rate before the termination. It may be seen that the calculation is consistent with the experimental results.

6. Discussion

6.1 Dimensionless groups

Physical meanings of the dimensionless groups for the gas cavity breakup are considered. Equation (26) is rewritten as follows:

$$Z_{b0} = k_b (Z_{b1})^{m_b} (Z_{b2})^{n_b} \tag{53}$$

where Z_b represents a dimensionless group and where

$$Z_{b0} \equiv \frac{(V_b)_0}{\bar{v}}$$

$$Z_{b1} \equiv \frac{\rho_\ell \bar{v}^2 d_b}{\sigma}$$

$$Z_{b2} \equiv \frac{d_b}{r_c}$$

The dimensionless group of Σ_{b1} is transformed by Eq. (16) as follows:

$$\Sigma_{b1} = \frac{\sqrt{\overline{\delta P^2}} \,/\, h_P}{\sigma \,/\, d_b} \quad \rightarrow \quad \frac{F_P}{F_S} \tag{54}$$

Hence, the dimensionless group of Σ_{b1} represents the ratio of the pressure fluctuation to the surface tension, as seen from Eqs. (18) and (21). The dimensionless group of Σ_{b2} is transformed by using Eq. (6) as follows:

$$\Sigma_{b2} = \frac{\rho_\ell \left(d_b \frac{v_d}{r_w} \right)^2}{\rho_\ell \frac{\bar{v}^2}{r_c} d_b} \quad \rightarrow \quad \frac{F_i}{F_c} \tag{55}$$

Hence, the dimensionless group of Σ_{b2} represents the ratio of the inertia force to the centripetal force, as seen from Eqs. (20) and (22).

The dimensionless group of Σ_{b0} represents the ratio between the average velocity of gas produced by the breakup of a gas cavity in the normal direction of the surface and the liquid velocity in the tangential direction.
The breakup rate may depend on the magnitude of the pressure fluctuations and on the frequency which may increase with increasing velocity of the liquid. The local velocity of liquid in the dimensionless group of Σ_{b0} may represent the contribution of the frequency on the breakup rate.

6.2 Centripetal force

The present model could describe experimental results by taking account of not only surface tension but also the centripetal force as the forces which opposed detachment of ripples. A comparison was made of a calculation without taking account of the centripetal force with experimental results and then no good correlation was obtained. Hence, the centripetal force is of importance for the mechanism of the gas cavity breakup behind a blockage as the opposing force.

The centripetal force is caused by the centrifugal force acting on the liquid, as discussed in section 2.4. The importance of the centrifugal force, and hence the centripetal force, can be also said from the equation of motion of liquid. The assumption of uniform angular velocity distribution (Assumption 3) gives the following equation from the equation of motion of liquid.

$$\rho_\ell \frac{v^2}{r} = \frac{\partial P_\ell}{\partial r} \tag{56}$$

where $\frac{\partial P_\ell}{\partial r}$ is the pressure gradient in the radial direction. Equation (56) is the equation of motion of liquid in the central vortex with uniform angular velocity distribution. The left-hand side of Eq. (56) represents the centrifugal force acting on the liquid. The ripples on the cavity surface move in the central direction by the local movement of liquid outwards due to the centrifugal force. Assumption 2 of the model, mentioned in Section 2.3, must be accepted if Assumption 3 is made.

6.3 Parametric study

In the present model the values of ε and ξ_b were used for the calculation as given values. However, these values might depend on the main flow velocity and blockage fraction. Therefore a parametric study is necessary to discover the influence of these values on the calculation of the transient behaviour of a gas cavity.

The influence of ε on the calculation of the residence time is shown in Fig. 11. With increasing ε, the re-absorption rate of bubbles into the cavity is increased. Hence the rate of decrease of the cavity radius is reduced and the residence time increases with increasing ε.

From the experiment of 21 % corner blockage in water [3], it may be said that the dependence of ε on the main flow velocity is small ($v_0 = 2 \sim 4.5$ m/s, $\varepsilon = 0.3 \sim 0.4$). However, the dependence of ε on the blockage fraction may be large, especially near $\frac{A_{Bf}}{A_{of}} = 1$.

The influence of ξ_b on the calculation of the residence time is shown in Fig. 12. With increasing ξ_b the surface area of the cavity where bubbles are produced is decreased. Hence rate of decrease of the cavity radius is reduced and the residence time increases with increasing ξ_b.

The experimental results for the dependence of the residence time on the main flow velocity could be described by the present model with a constant value of ξ_b. Hence the dependence of ξ_b on the main flow velocity may be negligible. However, the value of ξ_b may depend on the fraction of flow area blocked. Especially in the case that the blockage edge is in contact with the subassembly wall (corner blockage), the perimeter of the blockage edge protruding into liquid flow, and then ξ_b, changes with the blockage fraction.

6.4 Residence time in sodium

Though the constants of k_b, m_b and n_b were determined from experimental results in water, it may be possible to calculate the residence time of a gas cavity in sodium by using these values of the constants.

The predicted residence time of a gas cavity in sodium, based on the present model, is shown in Fig. 13, where the residence time in water is also shown for comparison. The breakup rate depends on physical properties of liquid density and surface tension. The liquid density of sodium is similar to that of water, but the surface tension of sodium is about two times higher than that of water. The high surface tension gives a long residence time because of the decrease of the breakup rate. Therefore the residence time of gas cavity in sodium becomes longer than in water.

6.5 Dependence of residence time on blockage size

The dependence of the residence time on the fraction of blockage is shown in Fig. 14 for the corner blockage and in Fig. 15 for the central blockage. As mentioned in Section 6.3, ε and ξ_b depend on the blockage size. However, the calculation in these figures used constant values of ε and ξ_b . As shown in these figures the residence time increases with the increasing fraction of the blockage and reaches a maximum, then decreasing. For the discussion on the dependence, ψ_{b3} of Eq. (50) which is a function of blockage fraction is transformed by using Eqs. (2) and (9) as follows:

$$\psi_{b3} = \left(\frac{4\pi^2}{\xi_w \xi_b}\right) \frac{r_w}{v_0^4} (\omega)^4 \tag{57}$$

where ω is the angular velocity of liquid in region 1 of the vortex and

$$\omega = \frac{v_d}{r_w} \tag{58}$$

The dependence of the angular velocity on blockage fraction is shown in Fig. 16. As shown in the figure the angular velocity initially decreases with an increasing fraction of blockage, falls to a minimum and then increases again. The decrease of the angular velocity is caused by the increase of the vortex radius, whereas the increase of the angular velocity is caused by the increase of the liquid velocity at the boundary of main stream and wake due to the flow obstruction. Therefore, it is found that the residence time has a maximum value for a blockage fraction since the angular velocity of liquid in the vortex, and hence the breakup rate of gas cavity, has a minimum value for same blockage fraction.

In reality, the dependence of ε on blockage size may be large.
The re-absorption rate affects the residence time and may depend on the velocity distribution in the wake, especially the reverse flow velocity near the wall. Hence, to predict the residence time for a high blockage fraction the dependence of ε on the blockage size must be taken into account. In this report, only the change of the angular velocity by the increasing blockage size and its influence on the residence time are pointed out.

7. Conclusion

A semi-empirical model has been developed to describe the transient behaviour of a gas cavity due to breakup behind a blockage in LMFBR subassembly geometry. The model satisfactorily correlates experimental results of the transient behaviour of gas cavity after the termination of gas injection.

The mechanism of gas cavity breakup is explained as follows: The pressure fluctuation of liquid due to the turbulence of the flow around the cavity causes ripples on the surface, which are then broken up to bubbles by the inertia force of liquid flow in the tangential direction. Against these forces, the surface tension and the centripetal force tend to prevent breakup and the resulting breakup rate depends on the balance of these forces. The centripetal force is of importance for the mechanism of the gas cavity breakup, because the liquid recirculates in the wake.

By extrapolation of the present model it is possible to predict the residence time of gas cavity in sodium. The residence time in sodium is higher than in water, decreasing with the increasing velocity of the main flow. Also, the prediction showed that the residence time had a maximum value for a blockage fraction since the angular velocity in the central vortex, and hence the breakup rate, had a minimum value for same blockage fraction. This may be significant for the safety aspects of LMFBR.

Acknowledgement

The author would like to express his gratitude to Dr. W. Peppler and Mr. F. Huber of the Institut für Reaktorentwicklung, Kernforschungszentrum Karlsruhe, for their valuable suggestions and discussions. The author wishes to express his thanks to Mr. A. Clare of C.E.G.B./England for his useful discussions.

Nomenclature

A_{Bf}	Blockage area (including fuel pins)
A_{of}	Total area of subassembly (including fuel pins)
A_t	Surface area of torus
F	Force
I	Intensity of turbulence
P	Pressure
δP	Pressure fluctuation
$\overline{V}_{ab}$	Re-Absorption rate
$\overline{V}_b$	Total breakup rate
$(\overline{V}_b)_o$	Breakup rate per unit area
$Z_{b0,1,2}$	Dimensionless groups
d_b	Bubble diameter
$f_{1,2}$	Arbitrary functions
k_b	Constant
m_b, n_b	Indices
r	Radial position in vortex
r_c	Cavity radius
r_i	Initial radius of gas cavity
r_{hc}	Hydraulic radius of sub-channel
r_w	Vortex radius
t	Time
$\bar{v}$	Time-averaged tangential velocity of liquid
v_d	Liquid velocity at the boundary of main stream and wake
v_t	Liquid velocity at the throat outside of the blockage
v_u	Reverse flow velocity near the wall
v_0	Main flow velocity

δv	Velocity fluctuation
$\psi_{b1,2,3}$	Functions
ε	Ratio of reverse flow velocity to main flow velocity
ζ	Ratio of re-absorption rate to total breakup rate
ξ_b	Geometrical factor for breakup region of gas cavity
ξ_f	Ratio of gas-liquid interface to total cavity surface including fuel pins
ξ_w	Geometrical factor of blockage
ρ	Density
σ	Surface tension
τ	Residence time

Suffix

b	Breakup or bubbles
g	Gas
l	Liquid

References

[1] R.M. Crawford, W.W. Marr, A. Padilla, Jr., and P.Y. Wang, "The Safety Consequences of Local Initiating Events in an LMFBR", ANL-75-73, (Dec. 1975)

[2] A.J. Clare, F. Huber, W. Till and W. Peppler, "Preliminary Results of the Temperature Distribution and Boiling Behaviour behind a Wall Blockage in a 169 Pin Bundle", 8. Liquid Metal Boiling Working Group Meeting, October 9, 1978, Mol

[3] Y. Fukuzawa, "Observations of the Behaviour of Gas in the Wake behind a Corner Blockage in Fast Breeder Reactor Subassembly Geometry", KfK 2820 (July 1979)

[4] P. Basmer, D. Kirsch and G.F. Schultheiß, "Phänomenologische Untersuchungen der Strömungsverteilung hinter lokalen Kühlkanalblockaden in Stabbündeln", KfK 1548 (Jan. 1972)

[5] D.P. Robinson, "Water Modelling Studies of Blockages with Discrete Permeabilities in an 11 Pin Geometry", AEEW-M 1484 (June 1977)

[6] A.M. Judd, "Measurements of Flow in an Air Model of a Partly Blocked Fast Reactor Subassembly", J.Br. Nucl. Energy Soc., Vol. 15, No. 1, p. 47-52, (Jan. 1976)

[7] C.V. Gregory and D.J. Lord, " Effect of Permeability on the Consequences of Local Blockages in Fast Reactor Subassembly", J.Br. Nucl. Energy Soc., Vol. 15, No. 1, p. 53-60 (Jan. 1976)

[8] P.B. Bird, W.E. Stewart and E.N. Lightfoot, "Transport Phenomena", p. 157, John Wiley and Sons, Inc. (1960)

[9] J.O. Hinze, "Turbulence", p. 242, McGraw-Hill Series in Mechanical Engineering

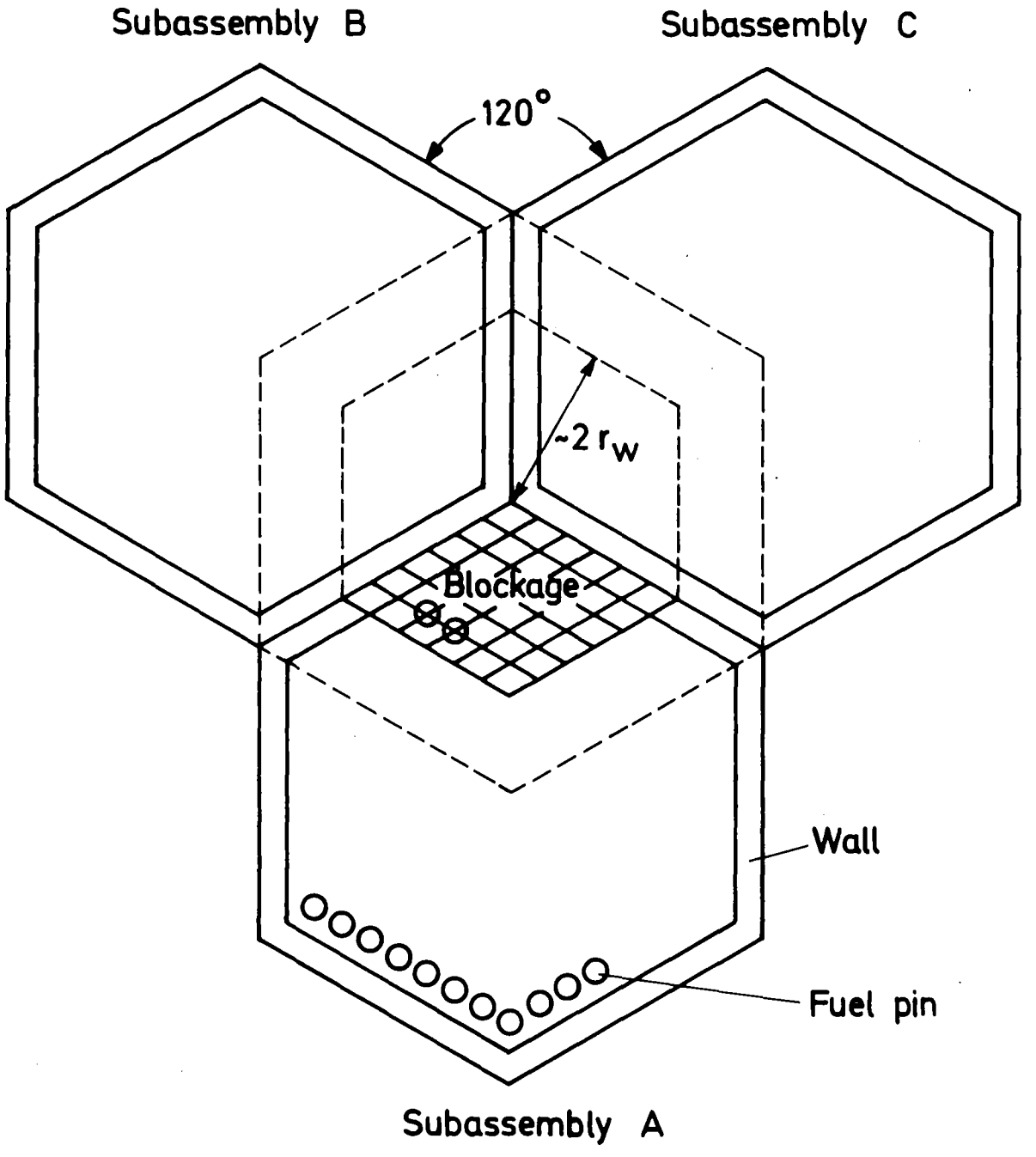

KfK

Fig.1 Cross section of the subassembly with a corner blockage

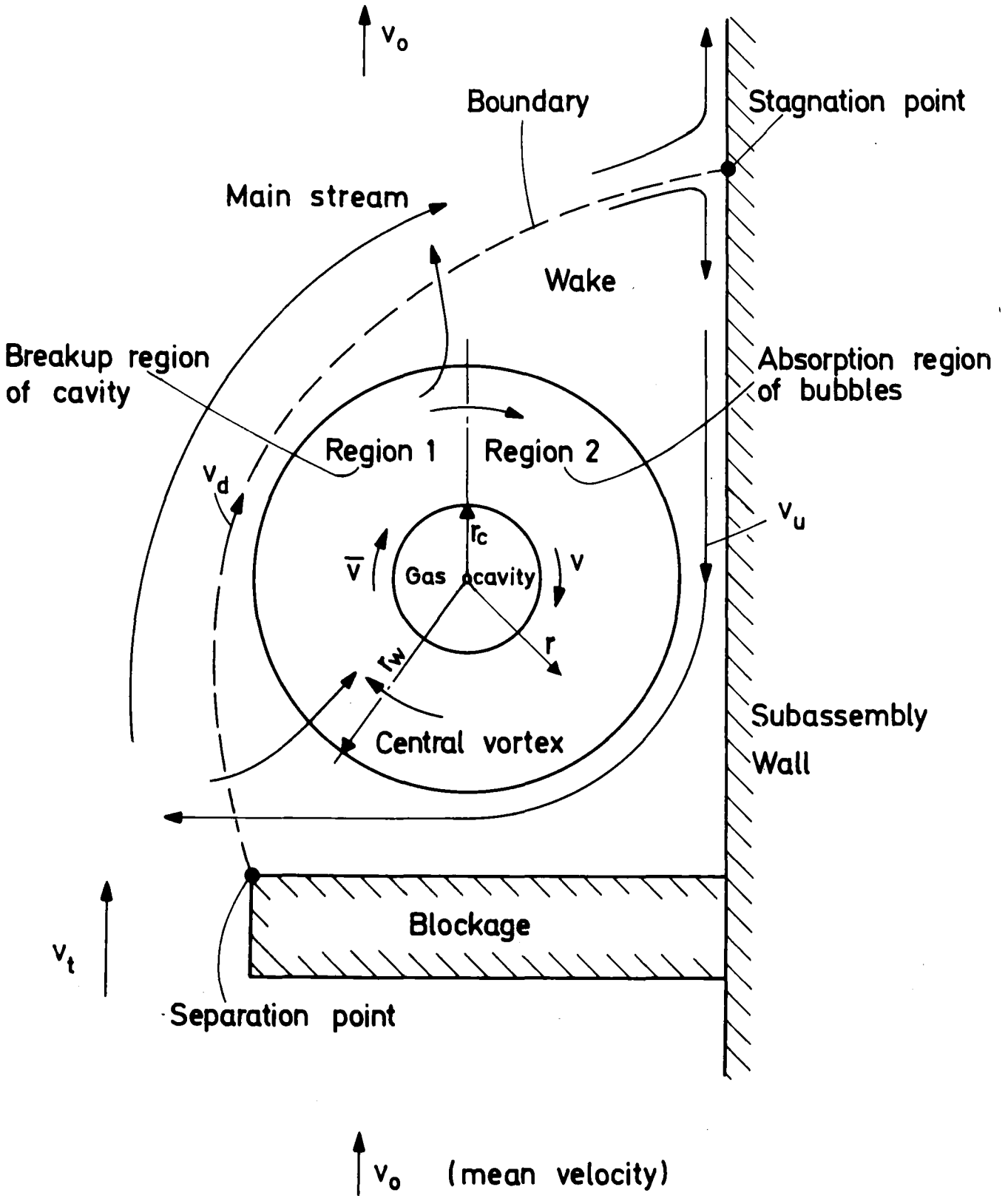

Fig. 2 Features of the model

Liquid pressure : fluctuates

$P_l = \overline{P_l} + \delta P \quad (\gtrless 0)$

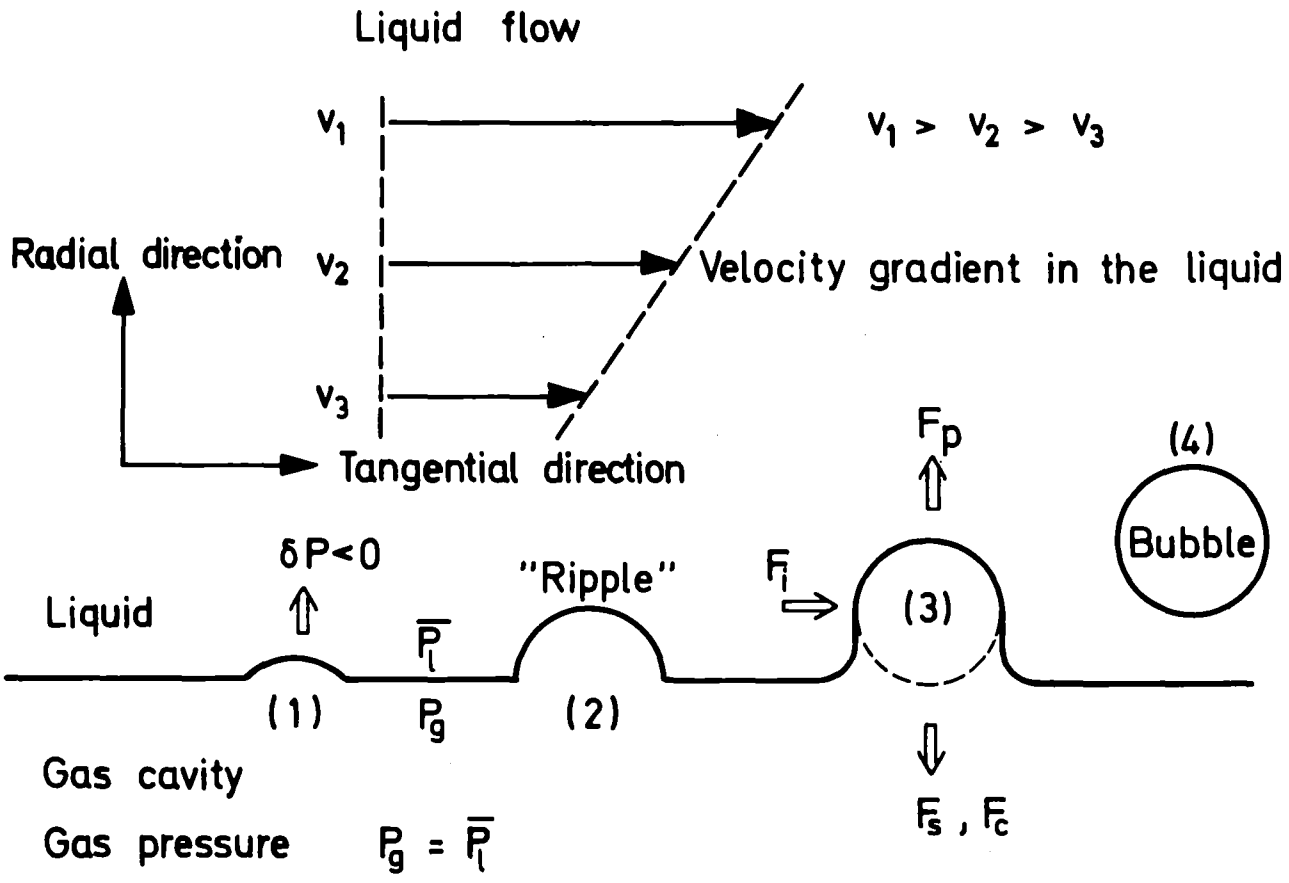

F_p : Pressure fluctuation

F_i : Inertia force

F_s : Surface tension

F_c : Centripetal force

KfK

Fig.3 Mechanism of gas cavity breakup

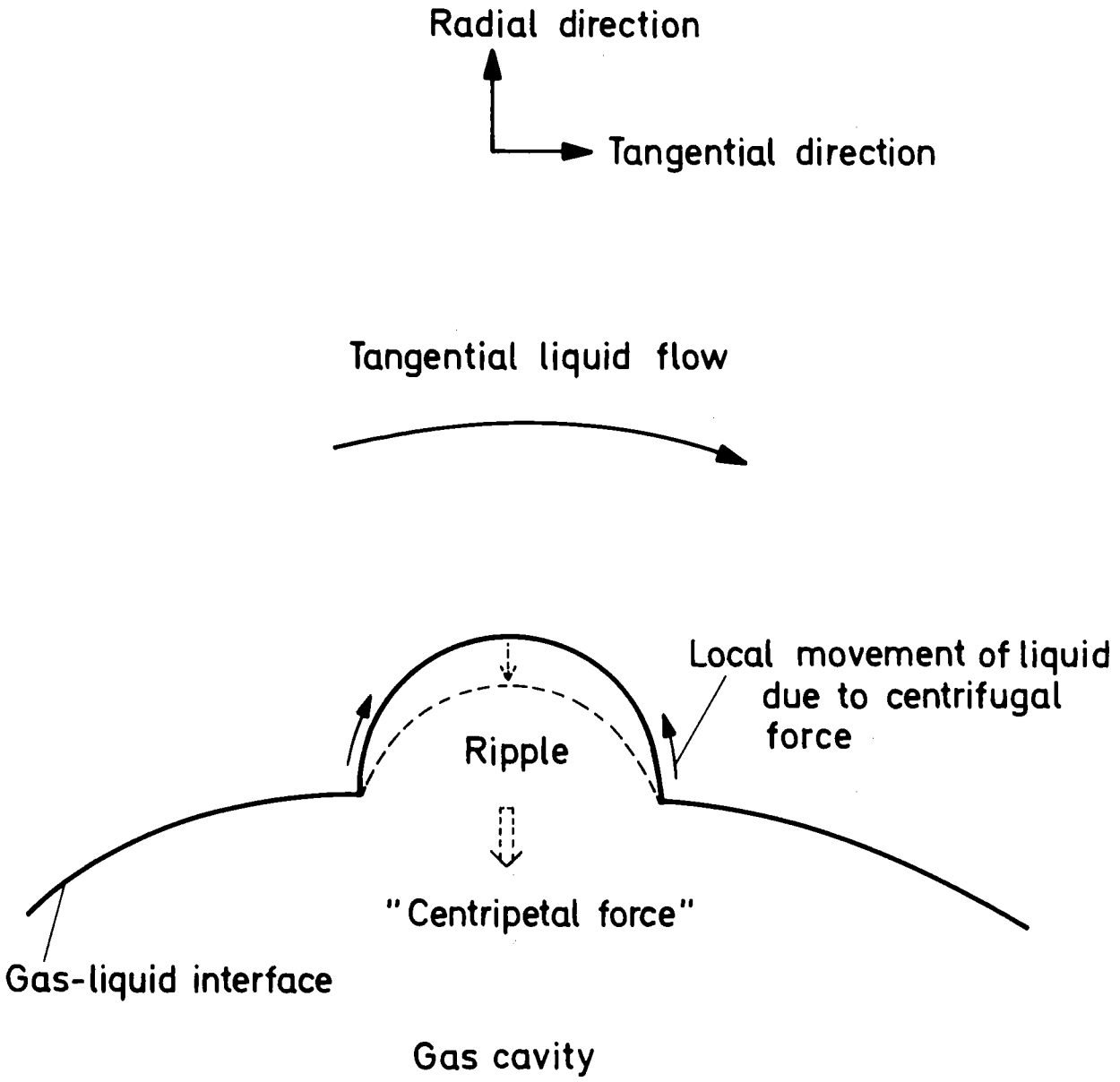

Fig.4 Opposition of ripple growth by centrifugal force acting on the liquid.

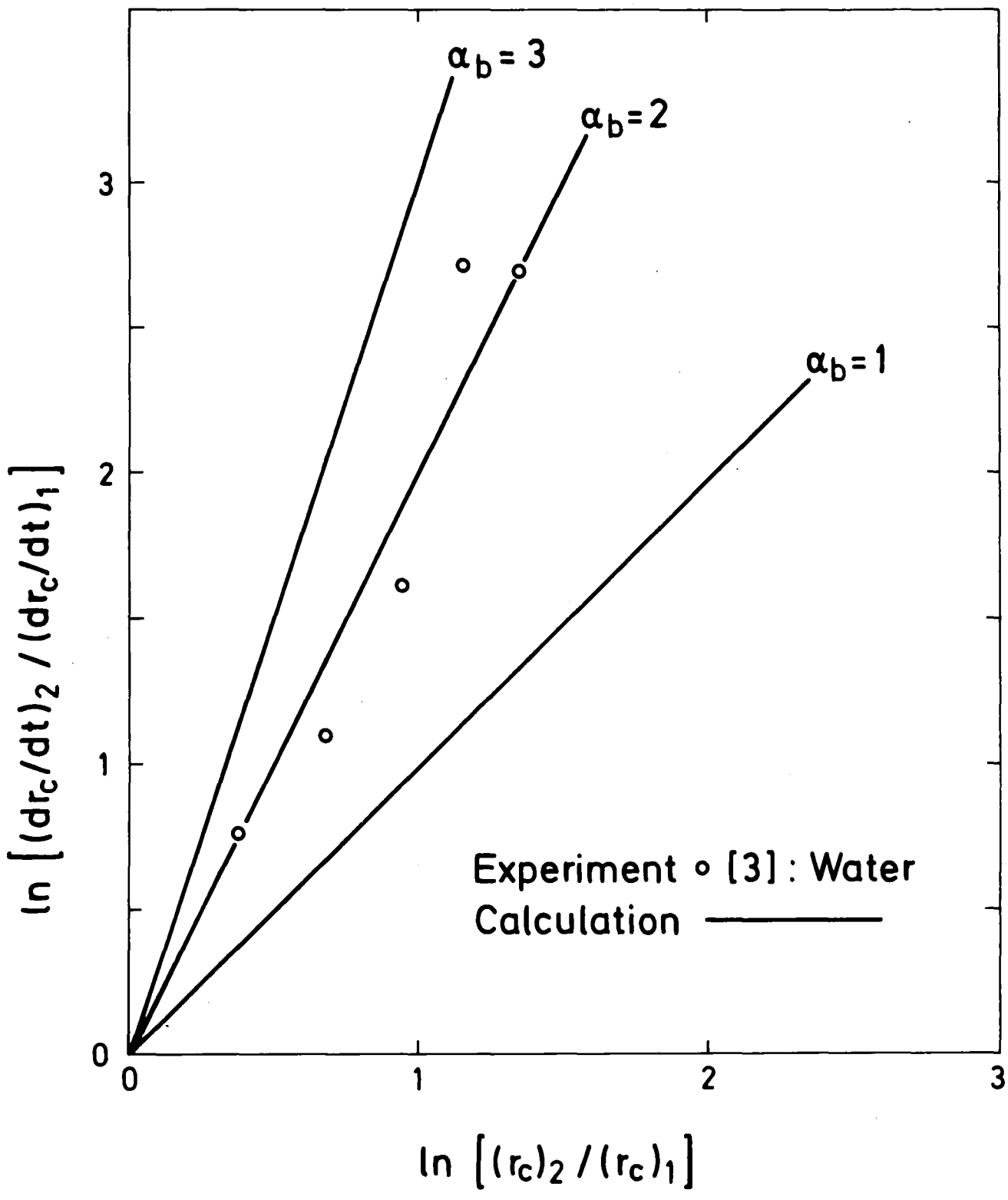

Fig.5 Determination of α_b

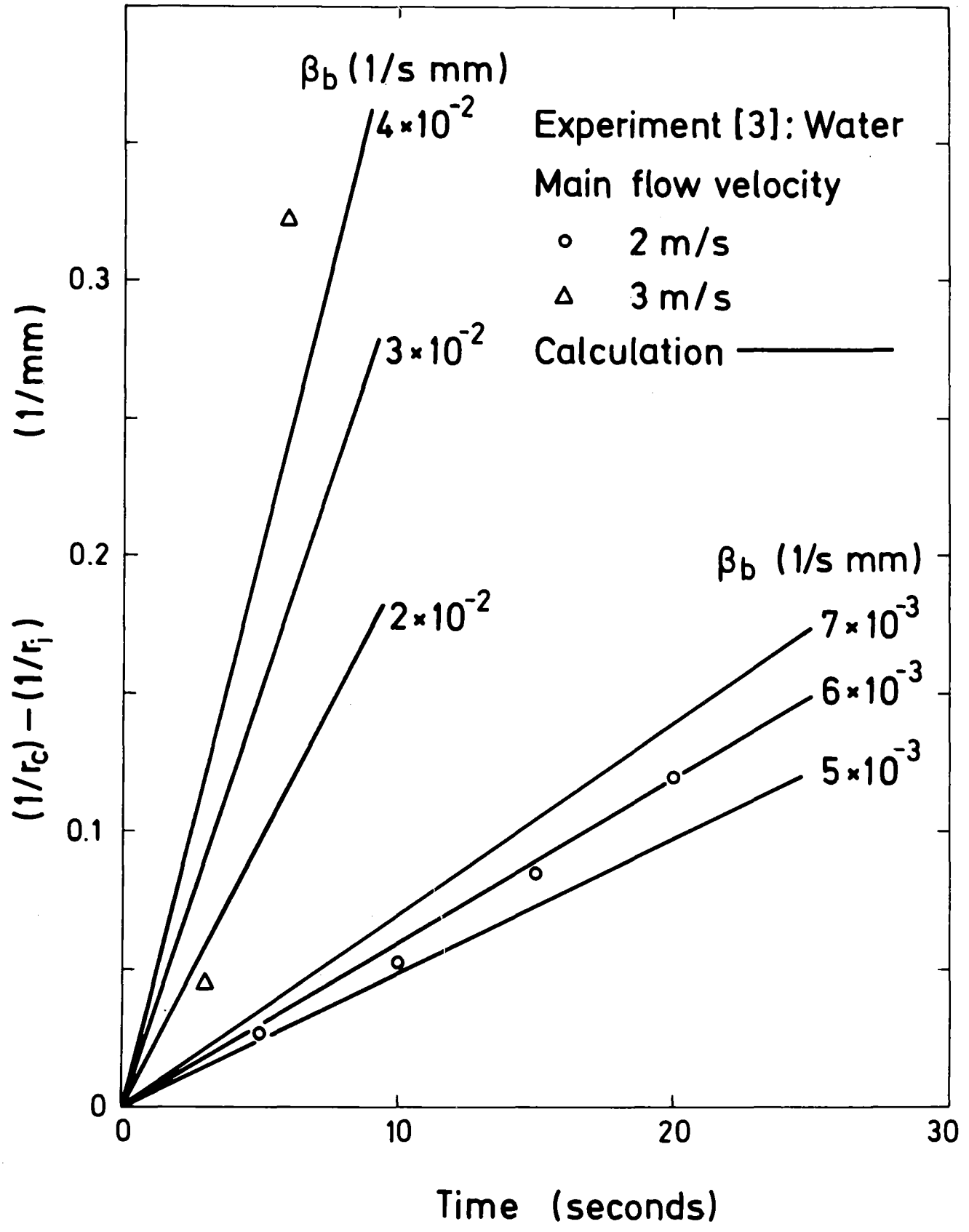

Fig.6 Determination of β_b

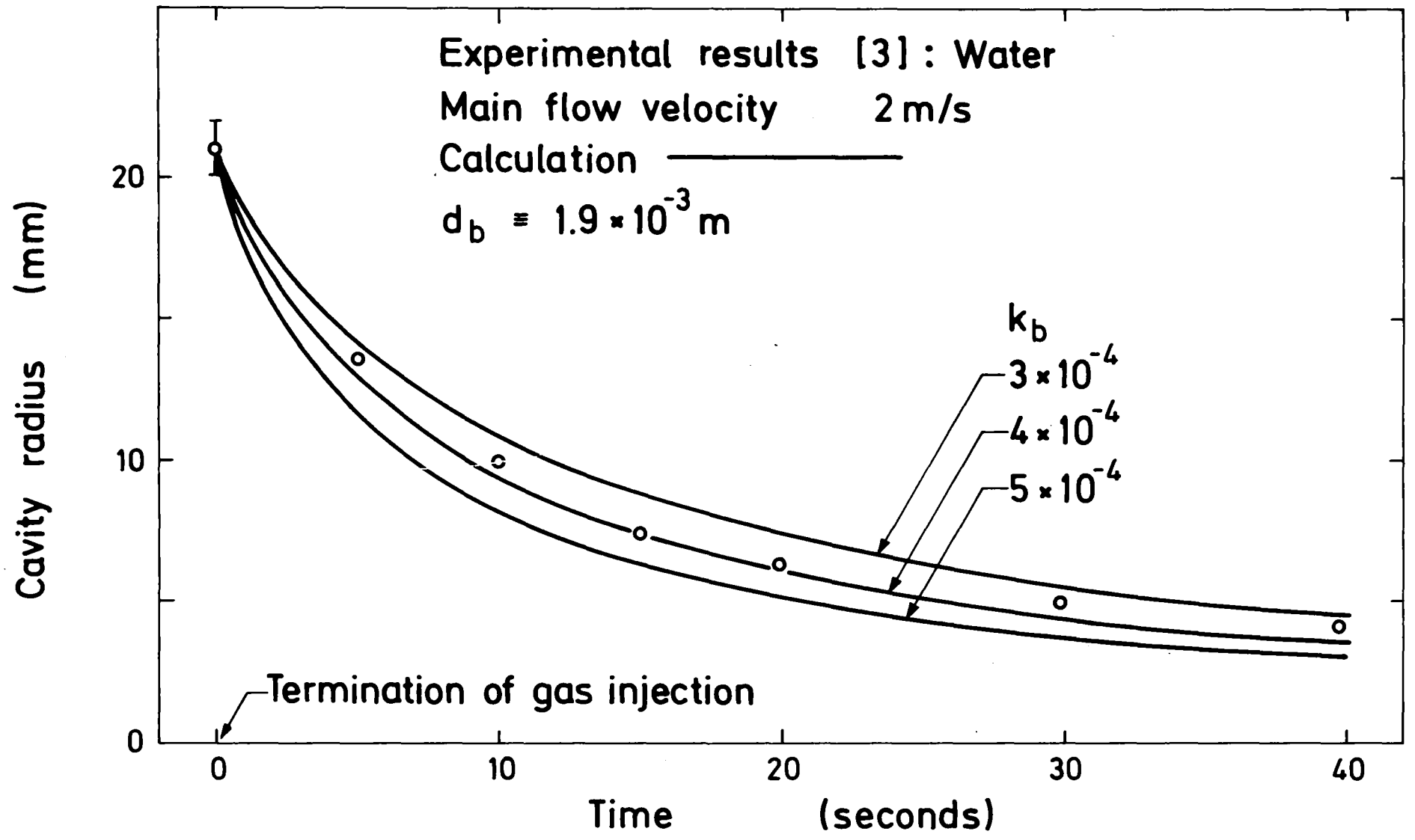

Fig.7 Determination of k_b

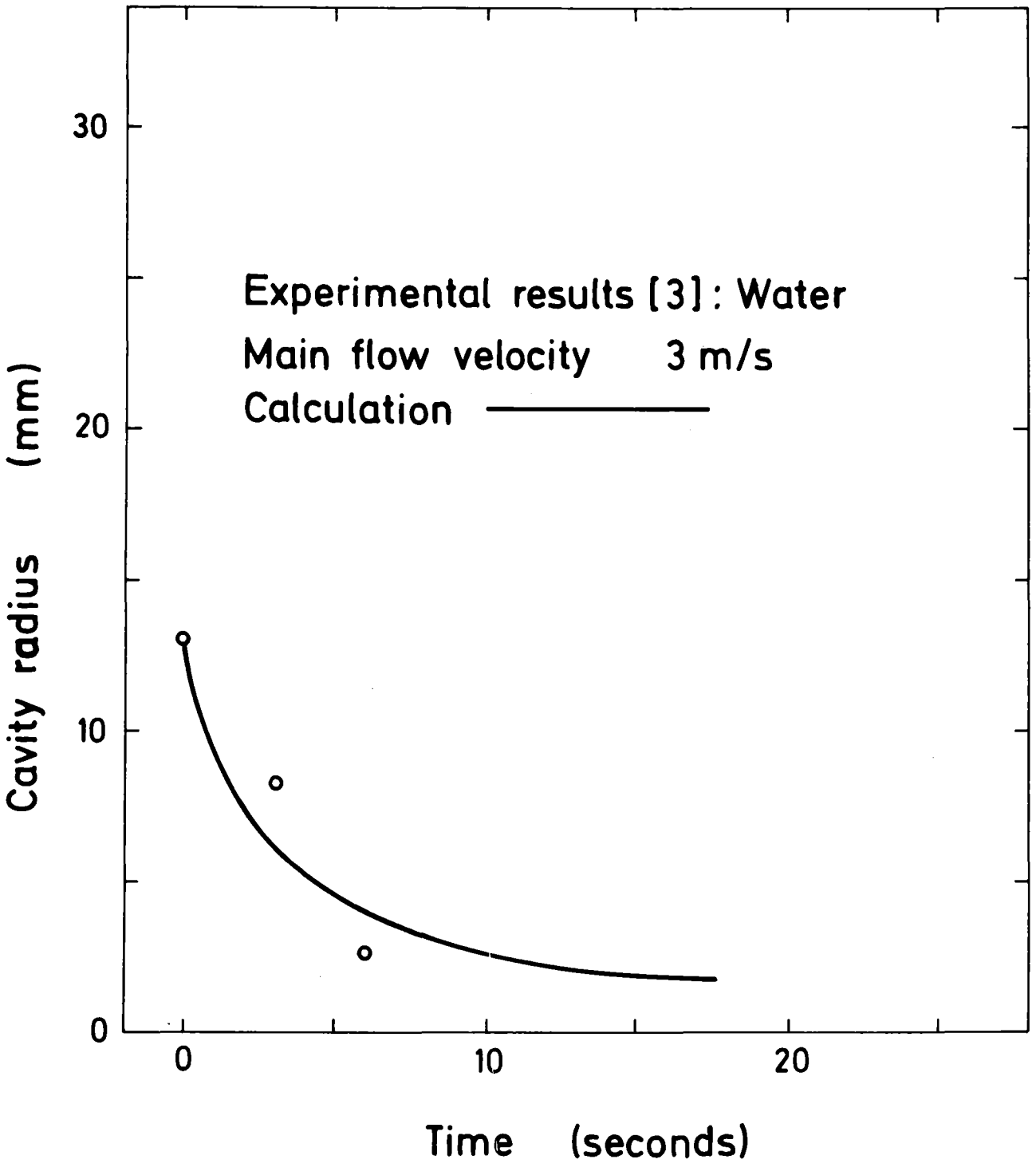

Fig. 8 Comparison of the calculation with experimental results for the change of cavity size

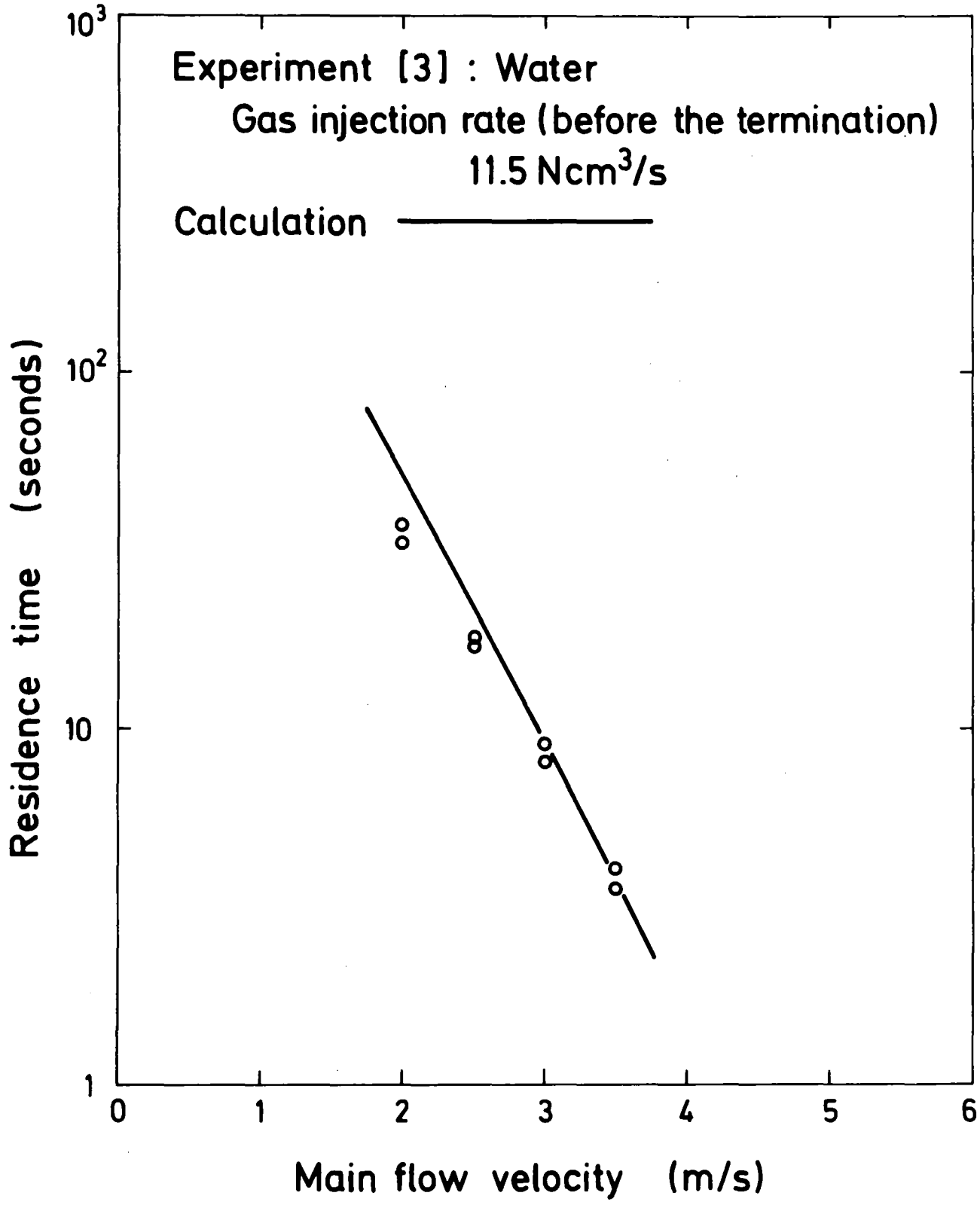

Fig.9 Comparison of the calculation with experimental results for the residence time

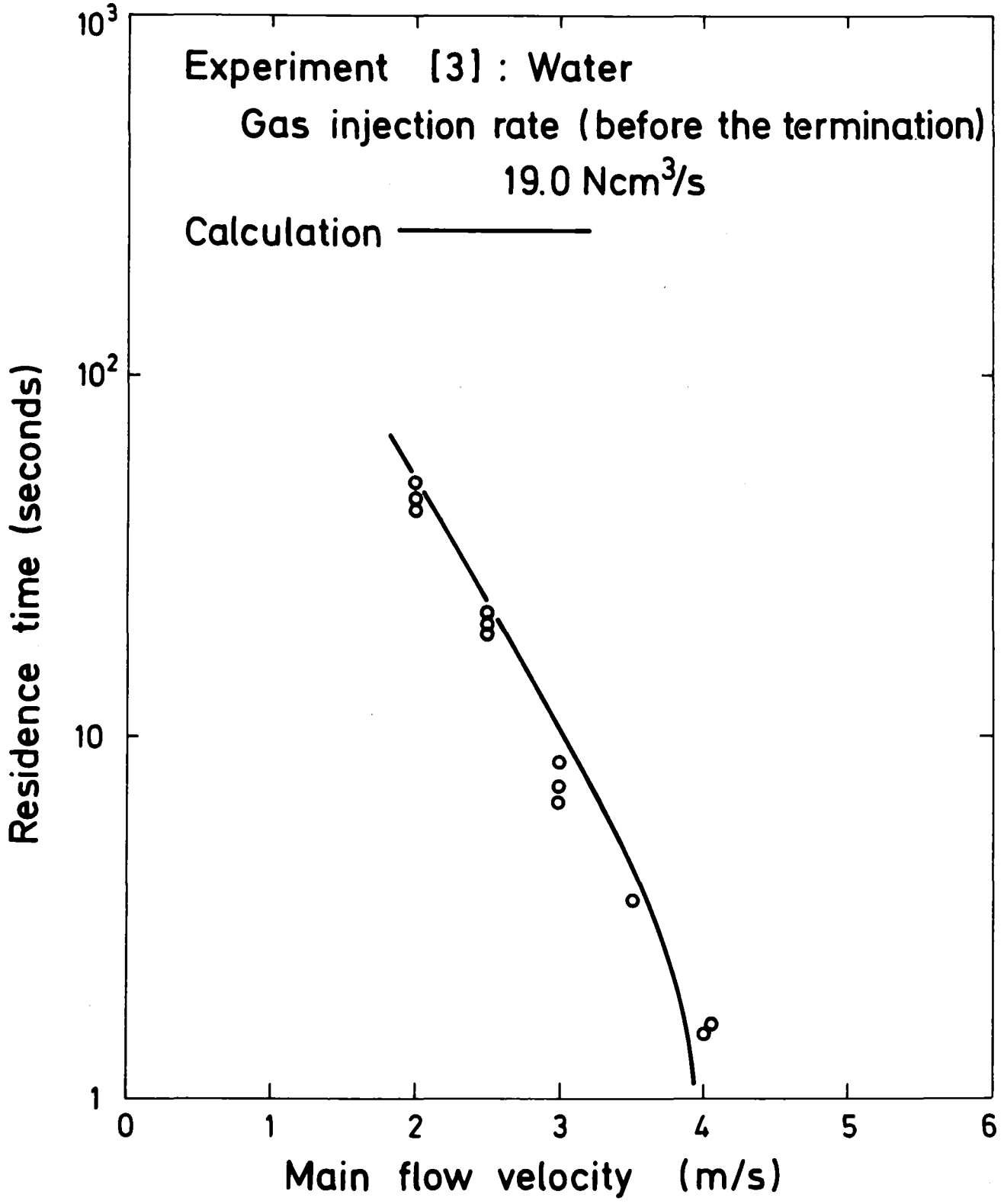

Fig.10 Comparison of the calculation with experimental results for the residence time

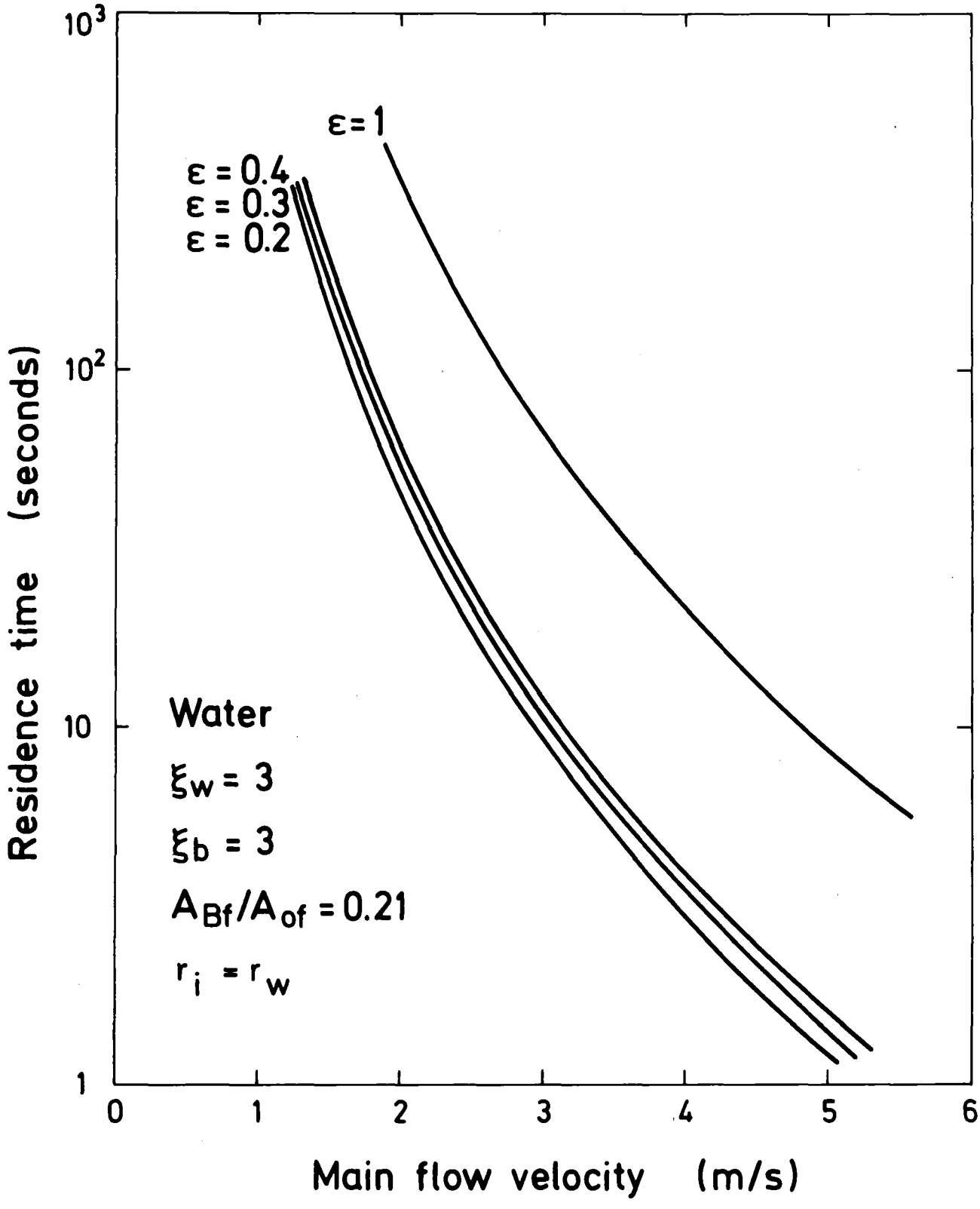

KfK

Fig.11 Influence of ε on the calculation of residence time

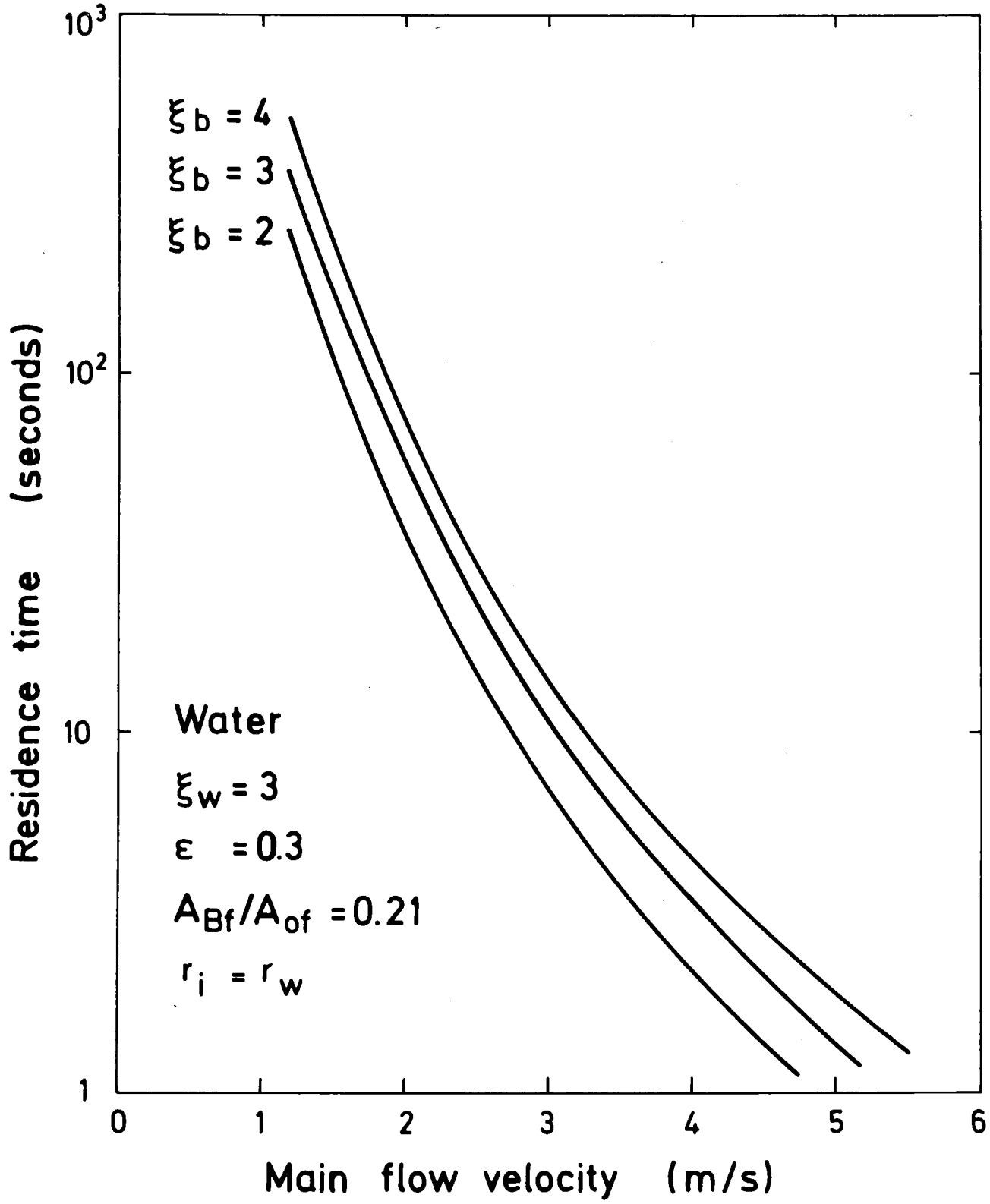

Fig.12 Influence of ξ_b on the calculation of residence time

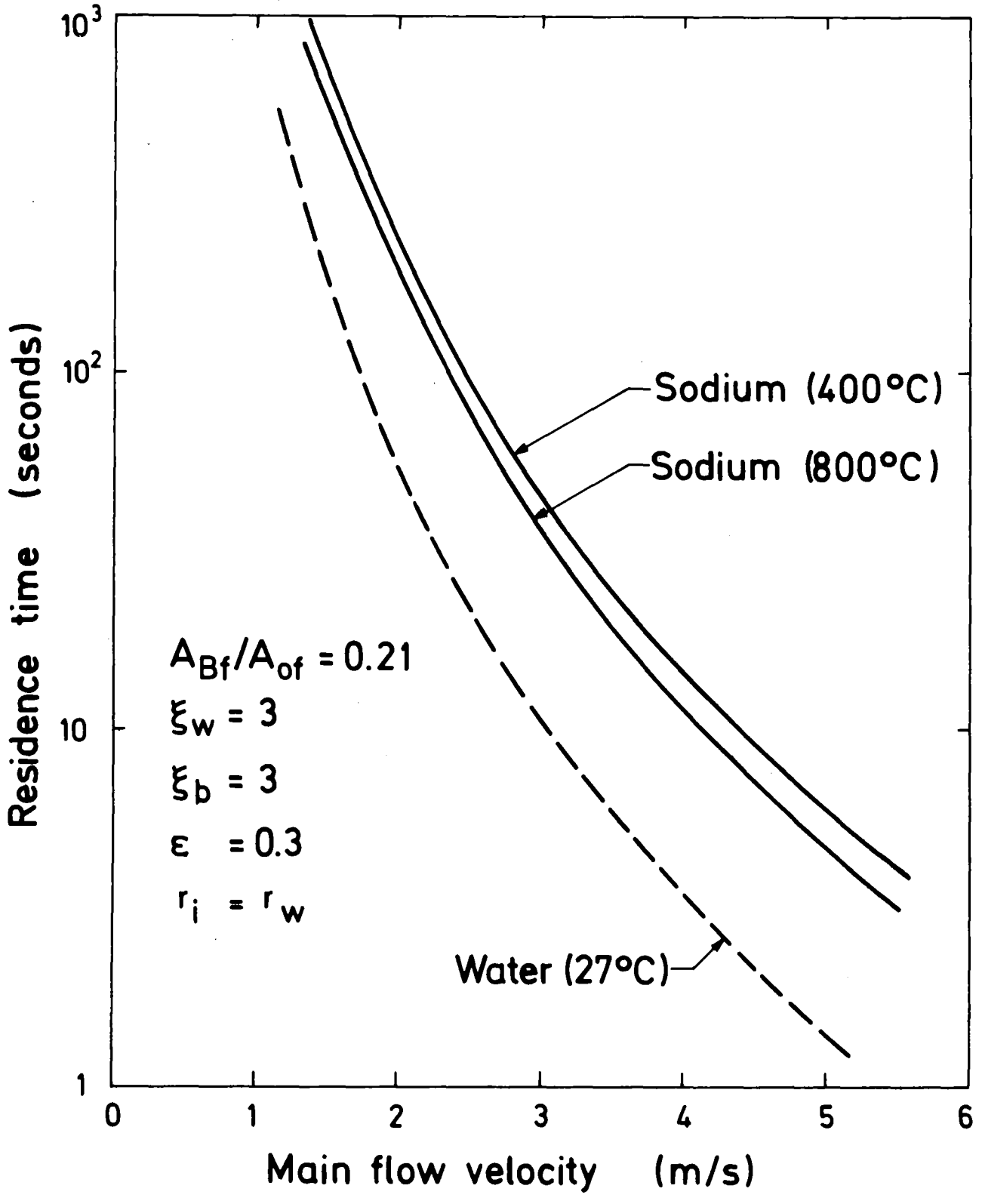

KfK

Fig.13 Residence time of gas cavity in sodium

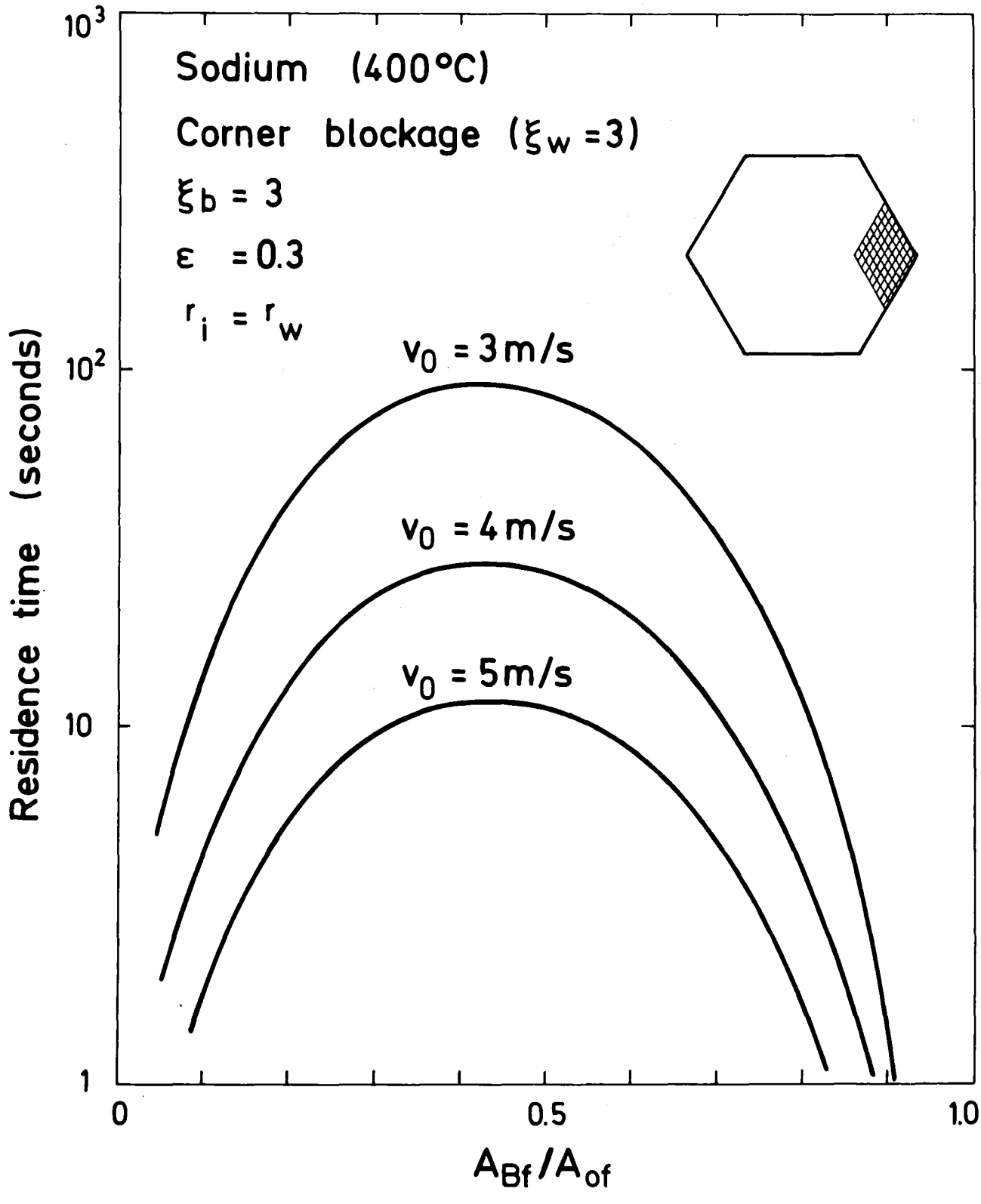

Fig.14 Dependence of residence time on blocked fraction for a corner blockage

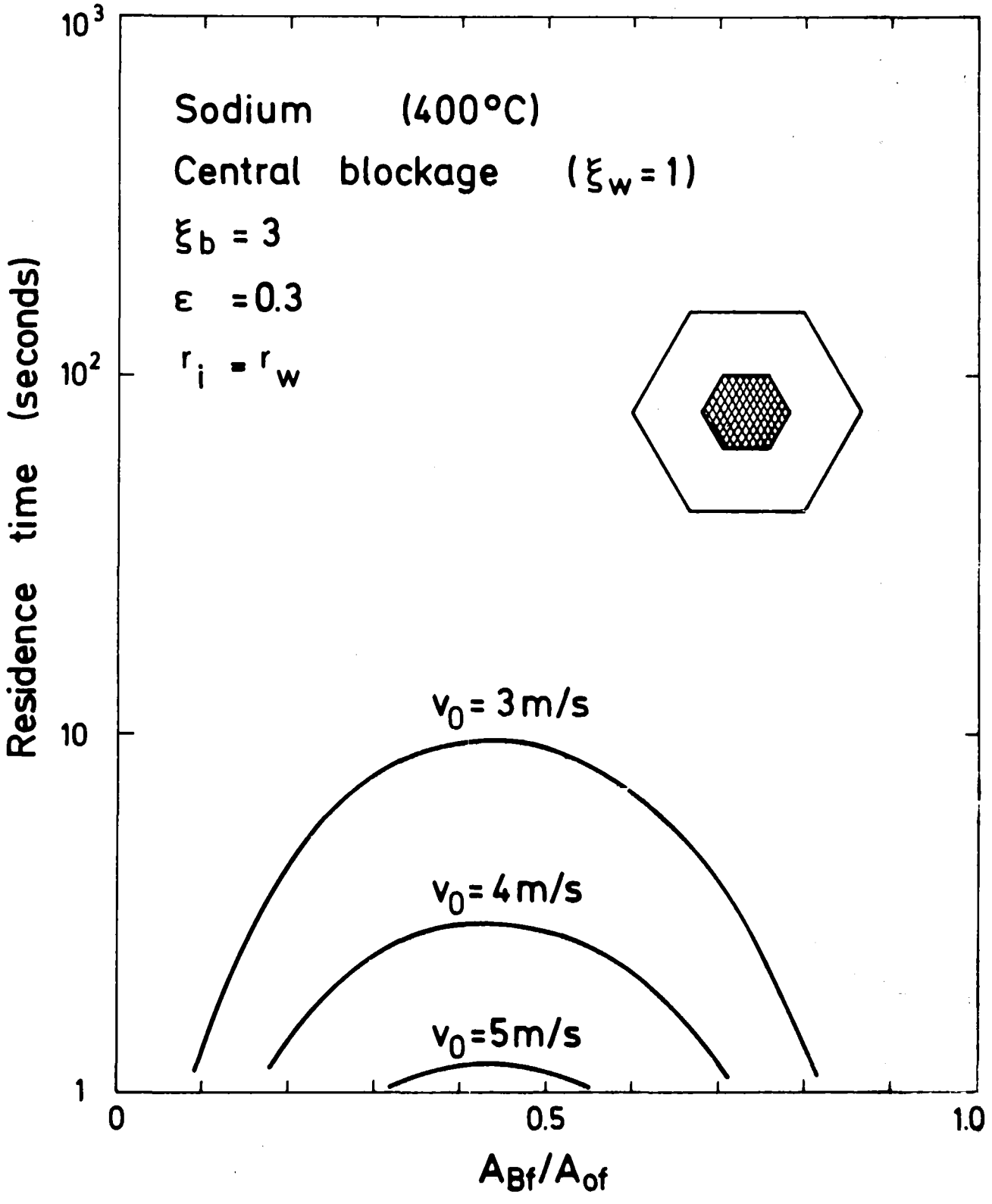

Fig.15 Dependence of residence time on blocked fraction for a central blockage

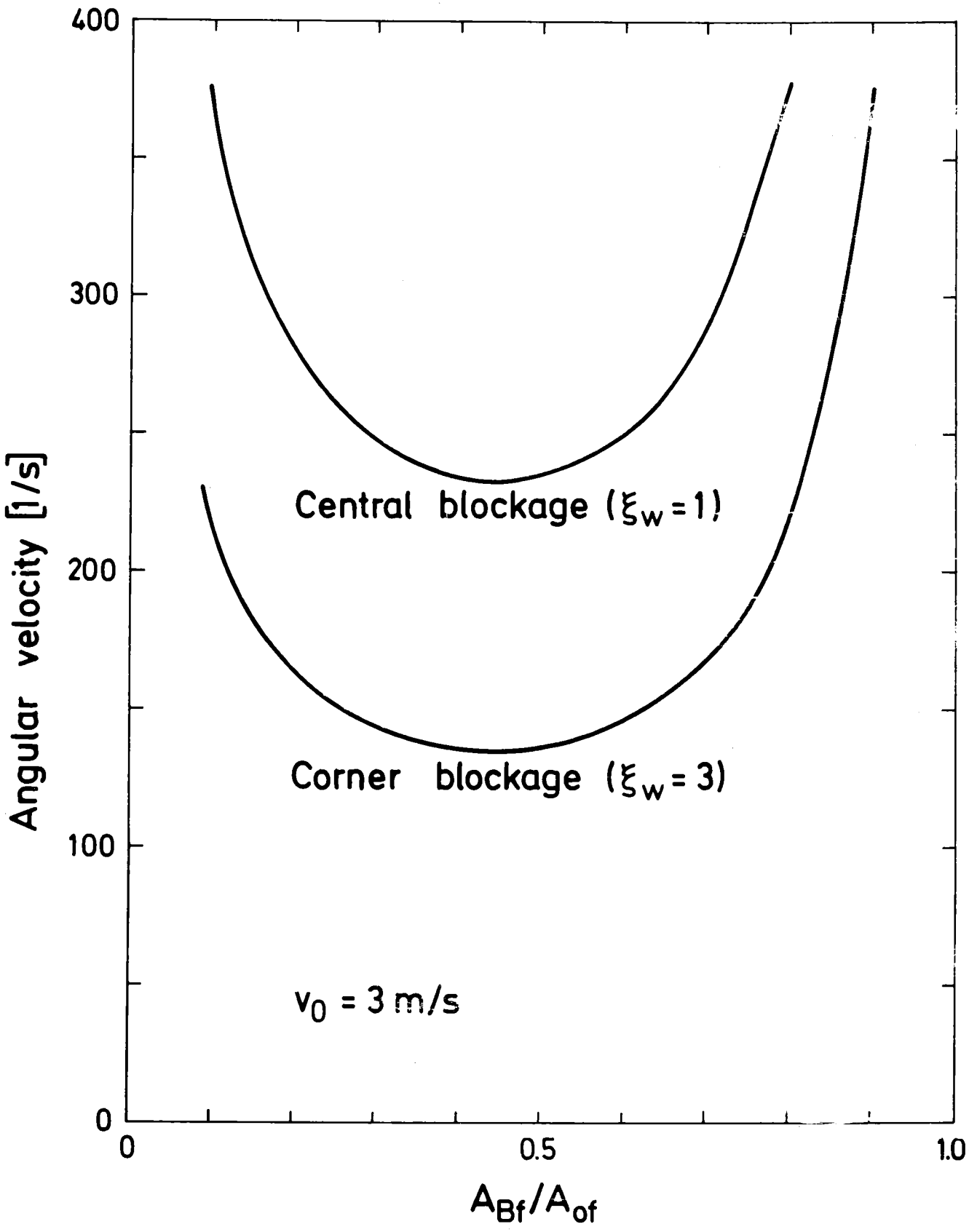

KfK

Fig.16 Dependence of angular velocity of liquid in the central vortex on blockage fraction